Sound & Vibration 2025, 59(2), 2767.
https://doi.org/10.59400/sv2767

Article

Optimizing acoustic vibration performance in Sitka spruce via grain inhomogeneity analysis: A hybrid approach of image processing and vibro-acoustic characterization

Siyuan Wang[1], Xiyue Li[1], Juncheng Zhang[1], Yaqing Guo[1], Lan He[1], Jing Zhou[1], Zhenbo Liu[1,*], Yinglai Huang[2,*]

[1] Key Laboratory of Bio-Based Material Science & Technology of Ministry of Education, Northeast Forestry University, Harbin 150040, China
[2] College of Computer and Control Engineering, Northeast Forestry University, Harbin 150040, China
*** Corresponding author:** Zhenbo Liu, liu.zhenbo@foxmail.com; Yinglai Huang, nefuyl@sina.com

CITATION

Wang S, Li X, Zhang J, et al. Optimizing acoustic vibration performance in Sitka spruce via grain inhomogeneity analysis: A hybrid approach of image processing and vibro-acoustic characterization. Sound & Vibration. 2025; 59(2): 2767. https://doi.org/10.59400/sv2767

ARTICLE INFO

Received: 10 February 2025
Accepted: 7 April 2025
Available online: 17 April 2025

Abstract: The inhomogeneity of the cross-sectional grain of Sitka spruce wood was analyzed using image processing techniques, and the influencing mechanism of this inhomogeneity on the acoustic vibration properties of the wood was investigated. The inhomogeneity of grain width was characterized by the average deviation of the growth ring width and latewood rate of the test specimens. The inhomogeneity of grain position distribution was characterized by the average deviation of the variation in growth ring width. The influence of the inhomogeneity of these grains on the acoustic vibration properties of the wood was investigated respectively. The results showed that as the inhomogeneity of the growth ring width and the growth ring width variation increase, the values of the specific modulus of elasticity (E/ρ), acoustic radiation quality constant (R), and acoustic impedance (ω) of the wood decrease, while the value of the loss angle tangent (tan δ) increases. As the inhomogeneity of the latewood rate increases, the values of E/ρ and R of the wood decrease, and the value of tan δ increases. The inhomogeneity of the latewood rate has no significant effect on ω. When the width of growth rings was between 0.14 cm and 0.17 cm while the deviation of the growth ring width ranged from 0.024 to 0.036 and the deviation of the width variation ranged from 0.016 to 0.020, the wood had relatively large values of E/ρ and R and a relatively small tan δ value, leading to better acoustic vibration performance. Similarly, when the latewood rate was between 15% and 20% and the deviation of the latewood rate ranged from 0.030 to 0.045, the wood had relatively large values of E/ρ and R and a relatively small tan δ value, leading to better acoustic vibration performance. This result provides more reference data for the rational selection of materials for musical instruments.

Keywords: wood acoustics; grain inhomogeneity; image-based texture analysis; vibro-mechanical properties; sustainable musical instrument materials

1. Introduction

Due to its excellent acoustic resonance and vibration frequency spectrum characteristics, wood is widely used in making soundboards of musical instruments [1]. In the context of the scarcity of wood resources, the continuous improvement of people's musical literacy, and the escalating demands for musical instruments, it is of great significance to evaluate and research the wood used in instrument-making.

How to efficiently select wood with excellent acoustic vibration performance is a concern for musical instrument manufacturers and also a direction in which relevant researchers keep conducting studies and making continuous improvements. In research, parameters such as specific dynamic elastic modulus, sound radiation

damping coefficient, acoustic impedance, logarithmic decrement rate, and loss tangent are often used to evaluate the acoustic vibration performance of wood [2,3]. Liu et al. [4] found that the oven-dry density of the wood used for fingerboards is all greater than 800 kg/m^3, and the acoustic performance requirements for fingerboard materials are lower than those for soundboards. Wan et al. [5] found that when the crack is close to the end of the wood and is relatively long, it has the greatest impact on the acoustic vibration performance of the wood. Zhang et al. [6] found that the periodic annular groove structure can be used to fine-tune the acoustic vibration performance of wood and coordinate the acoustic vibration characteristics among different wood specimens. Nop et al. [7] discovered that during the testing of the acoustic vibration performance of wood specimens varying in size, the anisotropy of wood makes the test results incomparable, and when the ratio of the length of the wood specimen to that of its width and thickness exceeds 48, the vibration behavior of the wood is close to the mathematical assumptions of isotropic and homogeneous materials. The Insulwood developed by Professor Hu Liangbing's research group at the University of Maryland is a kind of wood structure with high porosity [8]. It is manufactured by removing lignin and hemicellulose through high-temperature treatment and then undergoing low-cost environmental drying. This material integrates the characteristics of being renewable, having high porosity, high sound absorption, low thermal conductivity, and high mechanical strength. Moreover, its manufacturing process is efficient, economical, and scalable. It is expected to become a sustainable building material for improving building noise reduction and thermal regulation. This achievement provides a new idea for the sustainable utilization of wood in musical instrument manufacturing, and there may be possibilities to explore its application as an acoustic material for musical instruments in the future.

The influence on acoustic vibration performance of wood from wood grain, originating from the growth process of trees, is usually overlooked. Every year of a tree's growth gives rise to a growth ring, typically composed of earlywood and latewood. The alternative structure leads to obvious grain changes. In recent years, many studies on wood grain have focused on furniture design [9]. However, wood grain not only determines its aesthetics but also is one of the important criteria for evaluating wood quality [10,11]. Many studies have shown that the grain direction of wood has a significant impact on its acoustic vibration performance. As the grain angle increases, the dynamic elastic modulus and specific dynamic elastic modulus of spruce wood increase, and the tangent of the loss angle decreases. The acoustic vibration performance is the best when the grain angle is 90° [12,13]. Guiman et al. [14] found that there are significant differences in sound propagation among the three main cross-sections of spruce and maple. Among them, the radial section of the longitudinal specimen has the lowest sound absorption coefficient, which confirms the rationality of the luthiers' material selection. Liu et al. [15] found that the propagation speed of the sound vibration along the grain direction of the resonance panel is the highest, which is more than twice that in the cross-grain direction. The characteristics of the growth rings of wood are closely related to its acoustic performance. Liu et al. [16] found that when the growth ring width is between 1.0 mm and 1.5 mm and the latewood rate is approximately between 15% and 28%, the wood sample exhibits excellent acoustic vibration properties. Shen et al. [17,18] found that wood with

smaller coefficients of variation in growth ring width and latewood rate displays more excellent acoustic vibration performance. Wood of the Picea genus is the material of first choice for musical instruments such as violins, pianos, and guitars. Viala et al. [19] found that spruce with a serrated grain has less elastic property anisotropy and a higher vibration frequency compared to ordinary spruce. Upon reviewing the previous studies exploring the relationship between the grain and the acoustic vibration performance of wood, it is found that these studies often adopt the traditional method of manual measurement to obtain the data of grain width [16–18]. The operators need to distinguish the boundaries of the wood grain with the naked eye, and the process is rather cumbersome. With the development of computer technology, digital image processing technology has also developed rapidly. It has been widely applied in the field of wood science for wood defect detection [20,21], wood grain classification [22,23], and research on the microscopic structure of wood [24,25]. With the help of advanced edge detection algorithms, digital image processing technology can accurately capture the changes in the grain boundaries, clearly define the grain boundaries, and precisely identify them even in the face of extremely complex grain boundaries. This high-precision ability to distinguish boundaries can provide a reliable data foundation for research related to the wood grain. In recent years, studies using image processing methods to investigate the effect of wood grain on the acoustic vibration properties of wood have been relatively rare. Introducing image processing technology into the study of the relationship between wood grain and the acoustic performance of wood not only injects new content into the field of wood acoustics but also makes a positive contribution to supplementing the methods for the rational selection of materials for musical instruments.

Sitka spruce has been widely used in the musical instrument industry in recent years due to its straight grain, absence of knots and cracks, and characteristics of being lightweight, having the highest specific dynamic elastic modulus, relatively low internal friction, and strong anisotropy. In this study, we take Sitka spruce wood as the research object, analyze the cross-sectional grain of the wood specimen with the image processing function of MATLAB, and measure the grain information of the specimen manually by using Digimizer software. The average deviation is adopted to characterize the inhomogeneity of the grain width and the grain width distribution. The width of the growth ring, latewood rate, and inhomogeneity of the grain of the specimen are analyzed jointly to investigate the effect of the specimen grain on its acoustic vibration performance, with a view to providing theoretical guidance for the rational selection of materials for musical instruments.

2. Materials and methods

2.1. Test materials

Select the radial cut board of Sitka spruce (*Picea sitchensis*) as the test material, which has been air-dried for about a year, with a moisture content of approximately 6%. Process it into specimens with the dimension specifications of 200 mm (L) × 30 mm (R) × 8.6 mm (T). There are 44 specimens in total, and the surfaces of each specimen are polished to be smooth.

2.2. Test methods

2.2.1. Image processing and measurement

The scanner was used to accurately scan the cross-section of the specimen, and then a clear grain image of the specimen was captured. Based on feature extraction image recognition technology, the captured image was processed using the image processing function of MATLAB (version R2019b) [26–28], including grayscale conversion, filtering, and binarization, to ultimately obtain a binarized image of the specimen with a clear grain and an easy-to-resolve boundary. The specific process is as follows.

The imread function was used to load the original image. Then, MATLAB's built-in function rgb2gray was employed to conduct the grayscaling processing of the image and convert the RGB color image into a grayscale one. This function calculated the grayscale value through the weighted average method, which could better reflect the visual effect during the conversion from a color image to a grayscale one. After that, filter processing was carried out on the grayscale image. The medfilt2 function built in MATLAB was utilized to perform the median filtering operation, replacing the target pixel value with the median of the neighboring pixel values. This method could effectively remove random noise while better maintaining the edge and detail information of the image. Besides, it is simple to operate and easy to implement [29]. To further improve the image quality, the imgaussfilt function was used to implement Gaussian filtering for image smoothing, aiming to reduce the impact of high-frequency noise. In this study, the method of repeated trials was adopted. By observing and comparing the images before and after filtering, a proper standard deviation value was determined. This made it possible to remove high-frequency noise as much as possible while retaining the important details of the growth rings. The OTSU method [30] was adopted to automatically calculate the threshold for binarization. The OTSU method was implemented by the graythresh function, which calculated the interclass variance of all possible thresholds from the minimum to the maximum grayscale and selected the threshold that maximized the variance as the optimal threshold. The calculated thresholds were substituted into the imbinarize function to convert the grayscale image into a binary one, with the pixel values in the image being either 0 or 1, so as to highlight the characteristics of wood growth rings and the image grain.

Finally, the imshow function was used to view the images of each step, as shown in **Figure 1**. It can be seen that the binary image obtained after the above processing contains only two extreme values, black and white, which greatly simplifies the complexity of the image and highlights the contours of the wood grain for subsequent analysis.

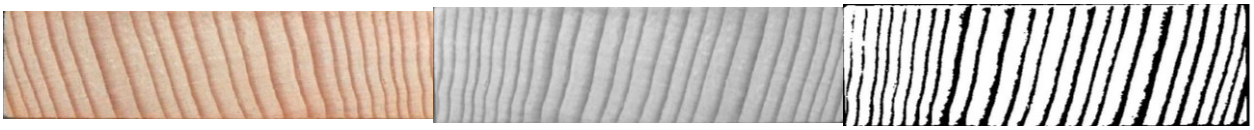

(a) **(b)** **(c)**

Figure 1. Specimen binarization. **(a)** Scanned image of specimen; **(b)** filter processing; **(c)** binary map.

The image processing flow chart is shown in **Figure 2**.

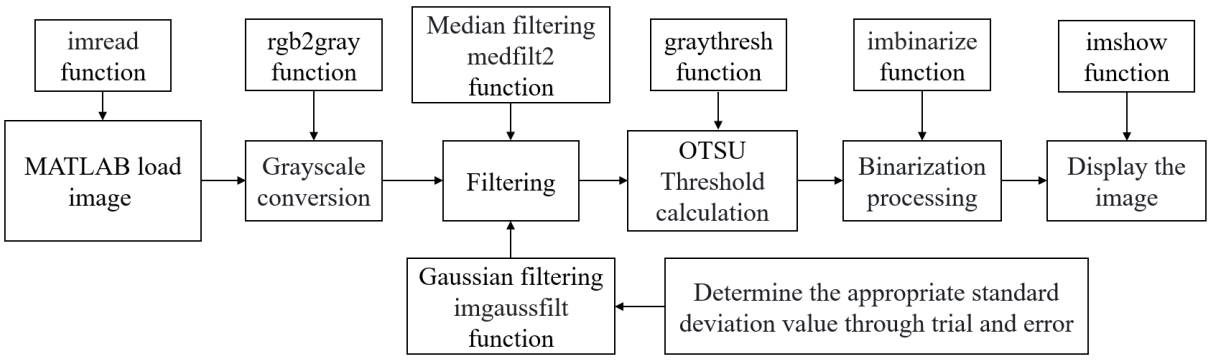

Figure 2. Image processing flow chart.

The growth ring width and latewood width of the specimen were measured manually using the image measurement software Digimizer on the binarized specimen image. Three specimens were randomly selected to compare the original image with the binarized image growth ring measurement results.

As illustrated in **Figure 3**, the test results are relatively close, indicating that the binarized image processing of wood grain is accurate and reliable. The binarized image diminishes the error originating from human eye recognition and is more intuitive than the original image to show the wood grain. This facilitates the differentiation between earlywood and latewood and subsequent measurement.

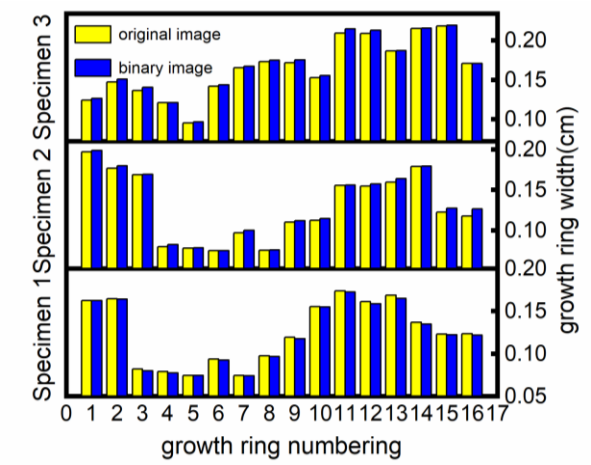

Figure 3. Comparison of growth ring width measurements between original and binarized images.

2.2.2. Measurement of cross-sectional grain

The image measurement and analysis software Digimizer (version 6.0.0.0) was used to manually measure the binary images of the specimen cross sections. After defining the unit of measurement, the width of the growth rings and the width of the latewood on the specimen cross-sections were measured. Measurements were taken at three locations, and the average values were calculated.

2.2.3. Characterization of grain inhomogeneity

The width of the growth ring and the latewood rate are used to characterize the grain width of the wood; the variation in the growth ring width is used to characterize the distribution of the wood grain. The growth ring width is the vertical distance between two adjacent ring boundaries. Growth ring width variation is the absolute value of the difference between the widths of two adjacent growth rings in the same specimen, used to characterize the changes in the distribution of growth ring width; the calculation method is given in Equation (1).

$$\Delta = |X_{i+1} - X_i| \tag{1}$$

where Δ is the change in growth ring width; X_i and X_{i+1} are the widths of the two adjacent growth rings.

The latewood rate is the percentage of latewood width to the width of the growth ring in which it is located and is given in Equation (2).

$$\text{latewood rate } (\%) = \frac{A}{X} \times 100\% \tag{2}$$

where A is the width of the latewood between the two adjacent ring boundaries and X is the width between the two adjacent ring boundaries.

The average deviation (*A.D.*) is the arithmetic mean of the absolute value of the deviation of each value in the series from its arithmetic mean, characterizing the degree of dispersion of a set of data. The coefficient of variation (*C.V.*) is also a statistic that reflects the degree of dispersion of the data and is used to compare two sets of data with different units or different means. Since the grain eigenvalues of wood have uniform units, it is more intuitive and easier to characterize the degree of grain heterogeneity by using the average deviation than by using the coefficient of variation. The average deviation of growth ring width and latewood rate is used to characterize the inhomogeneity of the size of the grain width of the specimen, and the amount of change in the growth ring width is used to characterize the inhomogeneity of specimen grain distribution. The larger the average deviation of the grain characteristic values is, the more inhomogeneous the grain is.

The mean values of growth ring width as well as latewood rate (μ) were calculated for each specimen, and Equation (3) is as follows:

$$\mu = \frac{1}{N}\sum_{i=1}^{N} X_i \tag{3}$$

where N is the total number of samples and X_i is the i-th growth ring width.

The average deviation (*A.D.*) is given by Equation (4) as follows:

$$A.D. = \frac{\sum|X_i - \mu|}{N} \tag{4}$$

2.2.4. Acoustic vibration performance testing

The test is based on the vibration theory of beams and adopts the test method of bending vibration for testing. Under free-boundary conditions at both ends, the back of the knife is used to strike the specimen. The vibration signal is transmitted to the dual-channel fast Fourier transform analyzer (FFT) through the transducer. Then the

vibration spectrum and vibration frequency are obtained, which are used to calculate the dynamic modulus of elasticity (E), the specific modulus of elasticity (E/ρ), the acoustic radiation quality constant (R), the acoustic impedance (ω), and the loss angle tangent ($\tan\delta$). The schematic diagram of the test is shown in **Figure 4**.

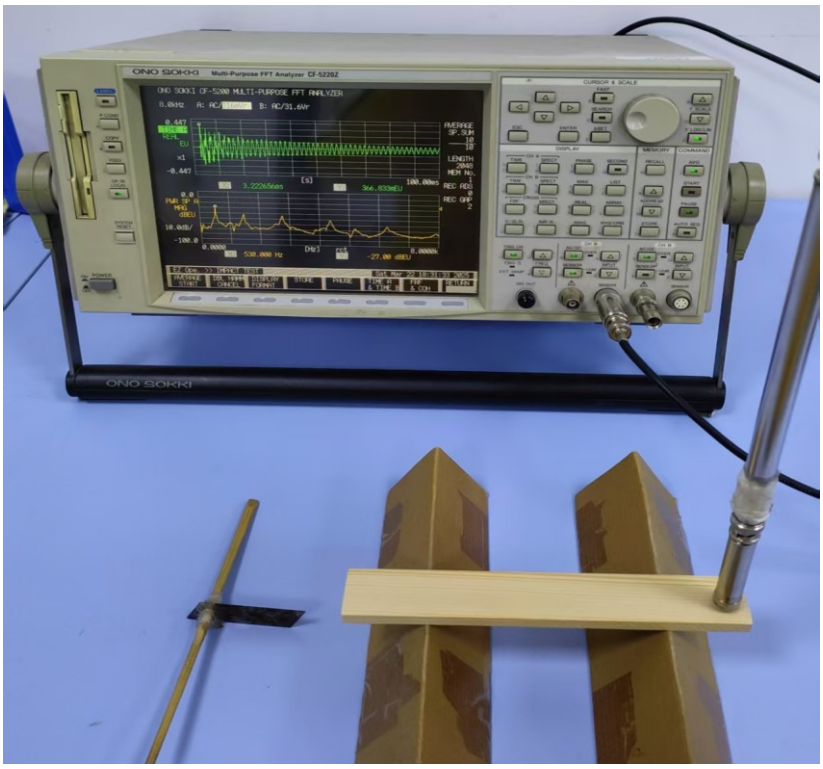

Figure 4. The schematic diagram of the test environment and the test.

The calculations of the dynamic modulus of elasticity (E), the specific modulus of elasticity (E/ρ), the acoustic radiation quality constant (R), the acoustic impedance (ω), and the loss angle tangent ($\tan\delta$) are given by Equations (5)–(9) as follows:

$$E = \frac{48\pi^2 \rho L^4 f^2}{m^4 T^2} \tag{5}$$

where E is the dynamic elastic modulus, also known as Young's modulus; ρ is the density of the specimen; L is the length of the specimen; f is the resonant frequency of the specimen; T is the thickness of the specimen; and m is the coefficient corresponding to the vibration order.

$$R = \sqrt{\frac{E}{\rho^3}} \tag{6}$$

where R is the acoustic radiation quality constant.

$$\omega = \sqrt{\rho E} \tag{7}$$

where ω is acoustic impedance.

$$\delta = \frac{1}{n} \ln \frac{A_i}{A_{i+1}} \tag{8}$$

$$\tan\delta = \frac{\delta}{\pi} \tag{9}$$

where δ is the logarithmic attenuation rate, and $\tan\delta$ is the loss angle tangent. A_i is the i-th amplitude of the time-domain sine wave of the specimen.

The schematic diagram of the test process is shown in **Figure 5**.

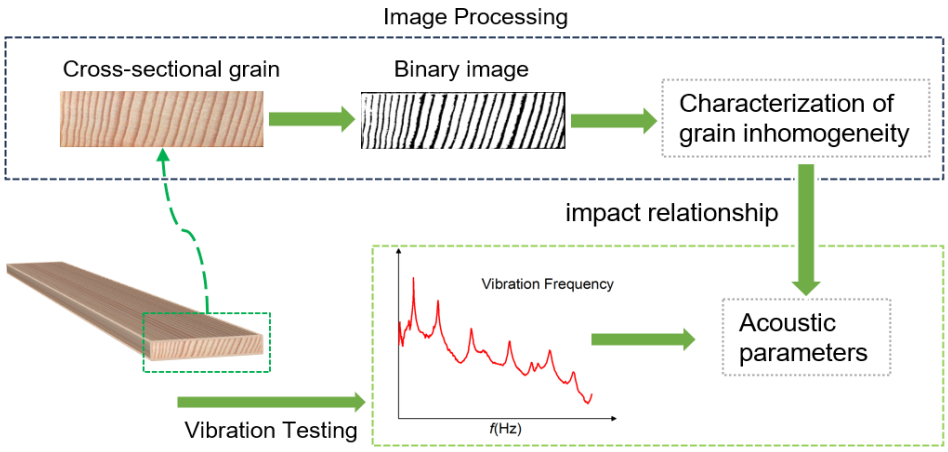

Figure 5. Schematic diagram of the test process.

3. Results and discussion

3.1. Effect of growth ring width inhomogeneity on acoustic vibration performance

Specific dynamic elastic modulus (E/ρ) represents the average dynamic elastic modulus of the cell wall of wood in the direction of the paragrain. It is an important physical index for the evaluation of the acoustic vibration performance of wood. Wood with a relatively high E/ρ can more effectively transfer vibration energy into the air under the same excitation conditions, thus producing a rich and bright timbre. The larger the E/ρ is, the better the acoustic performance of the wood is [31].

The relationship between the average deviation of the growth ring width and E/ρ is shown in **Figure 6a**, and the relationship between the growth ring width, the average deviation of the growth ring width, and E/ρ of the specimen is shown in **Figure 6b**.

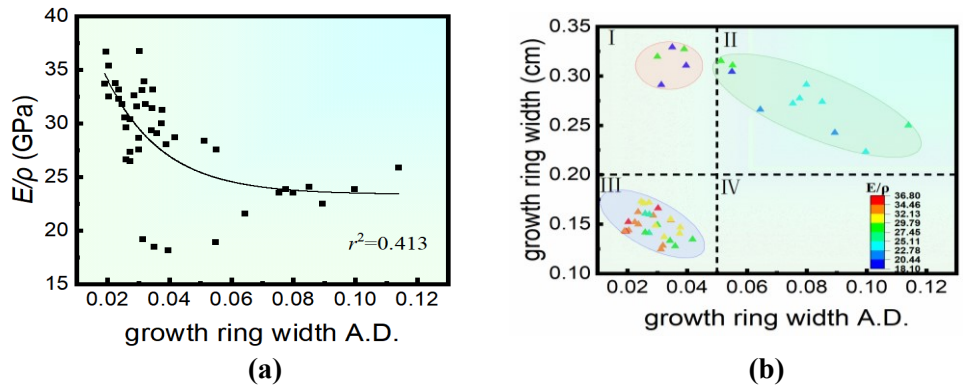

Figure 6. (a) Effect of growth ring width *A.D.* on E/ρ; **(b)** effect of growth ring width, growth ring width *A.D.* on E/ρ.

It can be seen in **Figure 6a** that the specimens with smaller average deviation of growth ring width have higher E/ρ values. The value of E/ρ shows a gradual downward trend as the inhomogeneity of the growth ring width of the specimen increases. The inhomogeneity of the growth ring width indicates that there is a significant difference in the width of the wood growth rings. In the area with wider growth rings, due to the relatively rapid growth of the wood, the cell walls are relatively thin, the cell cavities are larger, and the density of the wood is lower. In contrast, in the area with narrower growth rings where the growth is slower, the cell walls are thicker, the cell cavities are smaller, and the density of the wood is higher. As the inhomogeneity of the growth ring width of the specimen increases, the inhomogeneity of the internal structure and density distribution also increases. When the specimen vibrates, the vibration anisotropy in different regions increases, resulting in a low vibration energy transfer efficiency of the specimen. This is manifested as a decrease in the E/ρ value of the specimen and a reduction in the richness and brightness of the timbre. Since the fitting correlation coefficient in **Figure 6a** is relatively low, and considering that the growth ring width of the specimen will have a certain impact on it, the growth ring width of the specimen is added as a reference for joint analysis in **Figure 6b**. Divide the coordinate axes into four zones: Zone I growth ring width deviation ranges from 0.01 to 0.05, and growth ring width ranges from 0.2 cm to 0.35 cm; Zone II growth ring width deviation ranges from 0.05 to 0.12, and growth ring width ranges from 0.2 cm to 0.35 cm; Zone III growth ring width deviation ranges from 0.01 to 0.05, and growth ring width ranges from 0.1 cm to 0.2 cm; and Zone IV growth ring width deviation ranges from 0.05 to 0.12, and growth ring width ranges from 0.1 cm to 0.2 cm. From **Figure 6b**, it can be seen that the specimens are mainly concentrated in the three regions of I, II, and III, and the E/ρ values of the specimens in the III region are higher than those in the other two regions. It indicates that the specimens with smaller growth ring width and more uniform growth ring width have higher vibration efficiency. When the growth ring width of the specimen ranges from 0.14 cm to 0.17 cm and the average deviation of the width is between 0.02 and 0.036, the specimen reaches the maximum E/ρ value. During vibration, the sound features a richer and brighter timbre. This result aligns with previous research findings, which suggest that wood exhibits excellent acoustic properties when its growth ring width falls within the range of 0.08 cm to 0.25 cm [32]. It indicates that the research results are quite accurate, and the introduction of image-processing technology enables the precise extraction of the characteristic values of wood grain.

The acoustic radiation quality constant (R) represents the magnitude of the acoustic power radiated to the surrounding air when the wood vibrates and is an important parameter for characterizing the acoustic vibration performance of wood [33]. Wood with good R can generate abundant reflection and scattering when its sound propagates in the air, creating an auditory sense of spatiality and layering, which enhances the musical expressiveness.

The relationship between the average deviation of the growth ring width and R is shown in **Figure 7a**, and the relationship between the growth ring width, the average deviation of the growth ring width, and R of the specimen is shown in **Figure 7b**.

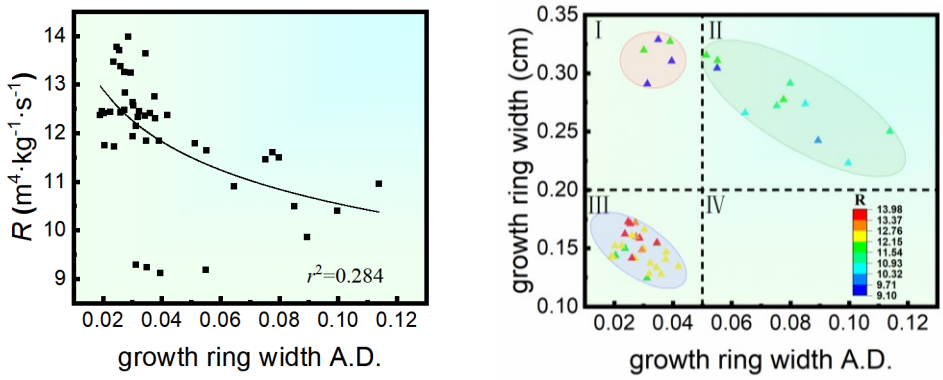

Figure 7. (a) Effect of growth ring width *A.D.* on *R*; **(b)** effect of growth ring width, growth ring width *A.D.* on *R*.

It can be seen from **Figure 7a** that the value of *R* shows a gradual downward trend as the inhomogeneity of the growth ring width of the specimen increases. As the inhomogeneity of the growth ring width of the specimen increases, the difference between the growth ring widths becomes larger, and the inhomogeneity of the cell structure and density distribution of the wood also increases. And the degree of anisotropy of the internal structure of the wood becomes larger. This leads to an increase in the differences in the vibration characteristics of the wood in different directions during vibration. These differences interact with each other, which is not conducive to the directional radiation of sound. In terms of acoustic vibration parameters, this is manifested as a gradual decrease in the value of *R* and a weakening of the sound expression ability of the wood. Since the fitting correlation coefficient in **Figure 7a** is relatively low, and considering that the growth ring width of the specimen will have a certain impact on it, the growth ring width of the specimen is added as a reference in **Figure 7b**. It can be seen that the *R* value of the specimens in zone III is larger, indicating that the specimens with smaller and more uniform growth ring widths radiate a larger acoustic power to the surrounding air during vibration. When the growth ring width ranges from 0.14 cm to 0.17 cm and the average deviation of the width is between 0.024 and 0.036, the specimen reaches the maximum value of *R*. During vibration, the sound has a stronger sense of space and hierarchy, and the sound expression is better.

The acoustic impedance (ω) of the wood represents the resistance of the wood to sound propagation; the smaller the value of ω, the smaller the resistance and the better the acoustic vibration performance [34].

The relationship between the average deviation of the growth ring width and ω is shown in **Figure 8a**, and the relationship between the growth ring width, the average deviation of the growth ring width, and ω of the specimen is shown in **Figure 8b**.

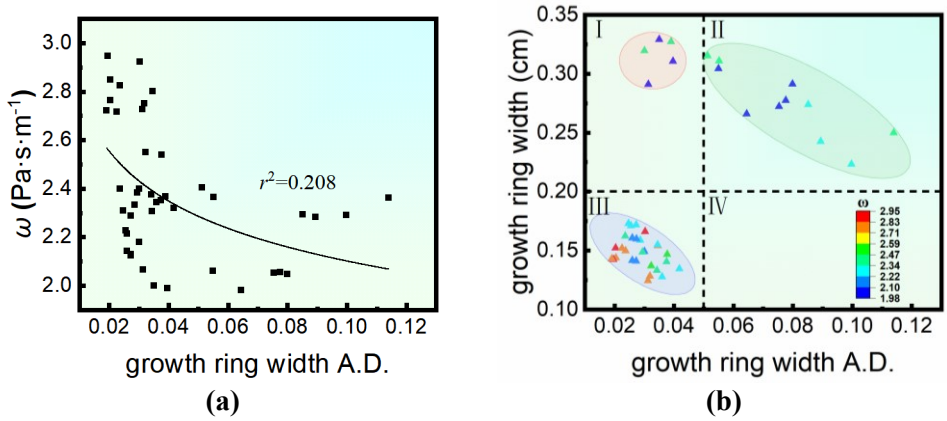

Figure 8. (a) Effect of growth ring width *A.D.* on ω; **(b)** effect of growth ring width, growth ring width *A.D.* on ω.

From **Figure 8a**, it can be observed that the value of ω shows a gradual downward trend as the inhomogeneity of the growth ring width increases. As the inhomogeneity of the growth ring width becomes larger, the difference between the growth ring widths becomes larger. The inhomogeneity of the internal structure distribution of the wood increases, resulting in a larger difference in density distribution. The value of ω is directly proportional to the overall density of the specimen [34]. A larger density difference may cause the overall average density of the wood to be relatively low, which is manifested as ω gradually decreasing as the inhomogeneity of the growth ring width increases. Since the fitting correlation coefficient in **Figure 8a** is relatively low, and considering that the growth ring width of the specimen will have a certain impact on it, the growth ring width of the specimen is added as a reference in **Figure 8b**. As depicted in **Figure 8b**, it can be noticed that the value of ω in regions I and II is smaller than that in region III, which indicates that the specimens with larger growth ring widths have less resistance to sound propagation. In zone III, when the growth ring width of the specimens is in the range of 0.14 cm to 0.17 cm and the average deviation of the width is in the range of 0.024 to 0.036, the value of ω of the specimens is relatively small. During vibration, the sound has a higher propagation efficiency, and the timbre is richer and brighter.

The wood loss angular tangent (tan δ) characterizes the ratio of the amount of heat loss per vibration cycle of the wood to the stored energy of the medium and is a quantity that describes the internal friction loss. The slow vibration attenuation of the wood can produce a long aftertone and sustain effect, making the timbre softer, warmer, and providing a comfortable auditory experience. The smaller the value of tan δ, the better the acoustic quality is [35].

The relationship between the average deviation of the growth ring width and tan δ is shown in **Figure 9a**, and the relationship between the growth ring width of the specimen, the average deviation of the growth ring width, and tan δ is shown in **Figure 9b**.

From **Figure 9a**, it can be observed that the value of tan δ shows a slight increasing trend as the inhomogeneity of the growth ring width increases. As the inhomogeneity of the growth ring width increases, the difference between the growth

ring widths becomes larger, indicating that the variability of the internal structure of the wood increases. When the wood vibrates, the variability of the vibration characteristics in different directions increases. These characteristics interact with each other, and the vibration energy is lost due to friction, resulting in an increase in tan δ. Since the fitting correlation coefficient in **Figure 9a** is relatively low, and considering that the growth ring width of the specimen will have a certain impact on it, the growth ring width of the specimen is added as a reference in **Figure 9b**. **Figure 9b** shows that the mean value of tan δ of specimens in zone III is smaller than that in zones I and II, indicating that specimens with smaller and more uniform growth ring width will have less internal friction loss and better acoustic vibration performance. Moreover, in zone III, when the growth ring width of the specimen is within the range of 0.13 cm to 0.17 cm and the average deviation of the width is within the range of 0.02 to 0.036, the value of tan δ of the specimen is the smallest. At this time, the vibration attenuation of the wood is slow, which can produce a longer lingering sound and a sustained effect, making the timbre softer and warmer and providing a comfortable auditory experience.

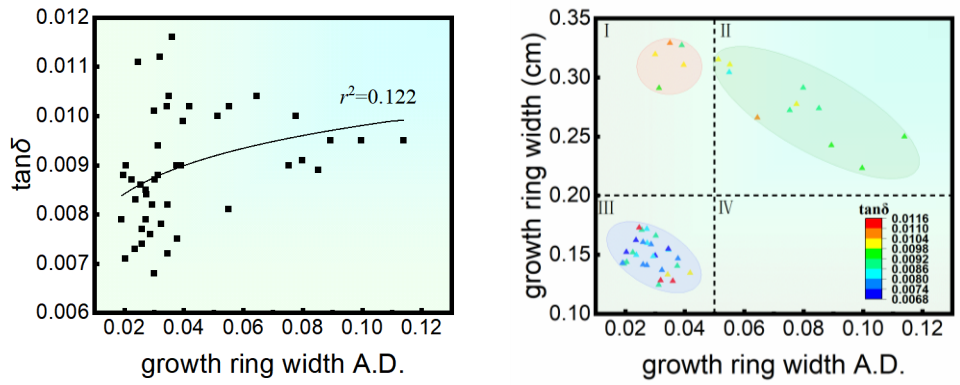

Figure 9. (a) Effect of growth ring width *A.D.* on tan δ; **(b)** effect of growth ring width, growth ring width *A.D.* on tan δ.

3.2. Effect of growth ring width distribution inhomogeneity on acoustic vibration performance

The relationship between the average deviation of the amount of variation in the growth ring width and E/ρ is shown in **Figure 10a**, and the relationship between the growth ring width, the average deviation of the amount of variation in the growth ring width, and E/ρ of the specimens is shown in **Figure 10b**.

It can be seen in **Figure 10a** that the value of E/ρ decreases with the increase of the average deviation of the amount of variation of the growth ring width, i.e., the value of E/ρ decreases as the degree of inhomogeneity in the growth ring width distribution increases. The increase in the inhomogeneity of the width distribution indicates that the difference in width between two adjacent growth rings becomes larger, and the difference in the internal cell structure and cell wall thickness also increases. Growth rings with thick cell walls and those with thin cell walls appear alternately, making the anisotropy of the wood vibration more significant. The interaction among them leads to a decrease in the energy transfer efficiency and a

reduction in the value of E/ρ. Since the fitting correlation coefficient in **Figure 10a** is relatively low, and considering that the growth ring width of the specimen will have a certain impact on it, the growth ring width of the specimen is added as a reference in **Figure 10b**. Divide the coordinate axes into four zones. In zone I, the deviation of the growth ring width variation amount ranges from 0 to 0.03, and the growth ring width ranges from 0.2 cm to 0.35 cm. In zone II, the deviation of the growth ring width variation amount ranges from 0.03 to 0.08, and the growth ring width ranges from 0.2 cm to 0.35 cm. In zone III, the deviation ranges from 0 to 0.03, with the growth ring width ranging from 0.1 cm to 0.2 cm. In zone IV, the deviation ranges from 0.03 to 0.08, and the growth ring width ranges from 0.1 cm to 0.2 cm. **Figure 10b** illustrates that the specimens predominantly cluster within zones II and III. This implies that when the growth ring width is narrow, the variation in width between adjacent growth rings tends to be minor. Conversely, when the growth ring width is wide, a more pronounced variation in width is typically observed. The average value of E/ρ of the specimens in region III is greater than that of the other three regions, which indicates that the specimens with smaller and more uniformly distributed growth ring widths possess a higher vibration efficiency. When the growth ring width is within the range of 0.14 cm to 0.17 cm and the average deviation of the width variation is within the range of 0.008 to 0.020, the value of E/ρ of the specimen is the largest. During vibration, the sound features a richer and brighter timbre.

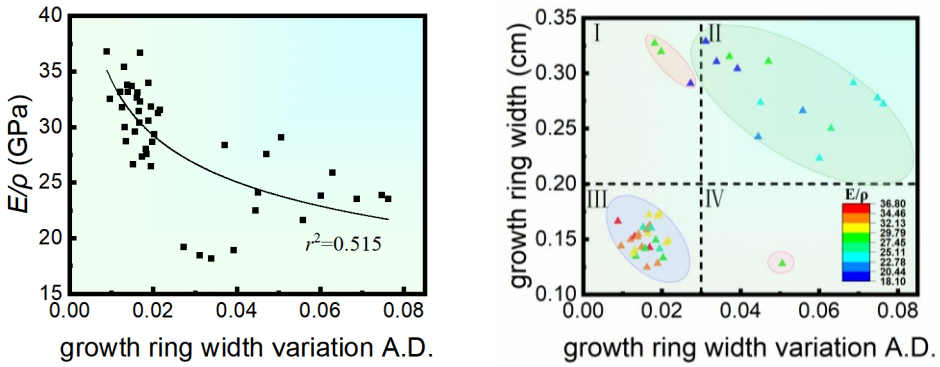

Figure 10. (a) Effect of growth ring width variation *A.D.* on E/ρ; **(b)** effect of growth ring width variation *A.D.* on E/ρ.

The relationship between the average deviation of the amount of variation in the growth ring width and R is shown in **Figure 11a**, and the relationship between the growth ring width, the average deviation of the amount of variation in the width of the growth ring, and R of the specimens is shown in **Figure 11b**.

As can be seen from **Figure 11a**, as the average deviation of the variation in growth ring width increases, the value of R shows a slight downward trend. The increase in the inhomogeneity of the variation in width makes the internal structure of the wood more disordered. During vibration, the significantly different vibration characteristics interact with each other, which is not conducive to the directional radiation of sound, resulting in a decrease in the R value of the wood. Since the fitting correlation coefficient in **Figure 11a** is relatively low, and considering that the growth ring width of the specimen will have a certain impact on it, the growth ring width of

the specimen is added as a reference in **Figure 11b**. As can be seen in **Figure 11b**, the *R* value of the specimens in zone III is larger than that of the specimens in the other three regions, indicating that specimens with a smaller growth ring width and a more uniform distribution radiate a greater acoustic power to the surrounding air during vibration and have better acoustic performance. In zone III, the specimens with a growth ring width in the range of 0.14 cm to 0.18 cm and an average deviation of the variation in width in the range of 0.016 to 0.020 have the largest *R* value. During vibration, the sound has a stronger sense of space and hierarchy and better sound expression.

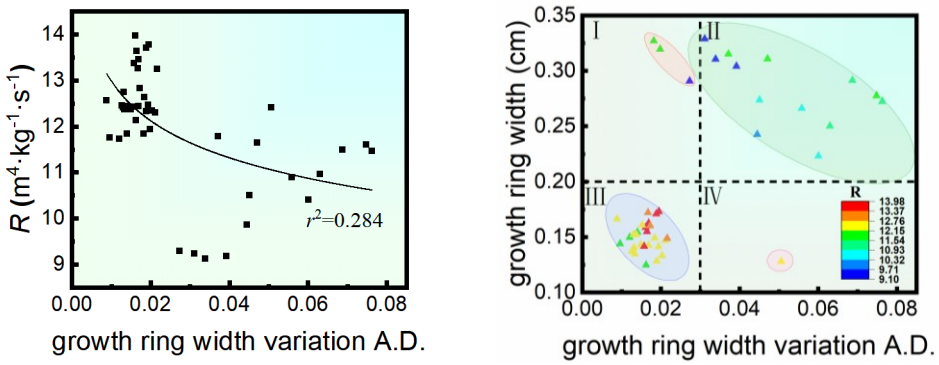

Figure 11. (a) Effect of growth ring width variation *A.D.* on *R*; **(b)** effect of growth ring width variation *A.D.* on *R*.

The relationship between the average deviation of the amount of variation of the growth ring width and ω is shown in **Figure 12a**, and the relationship between the growth ring width, the average deviation of the amount of variation of the growth ring width, and ω of the specimen is shown in **Figure 12b**.

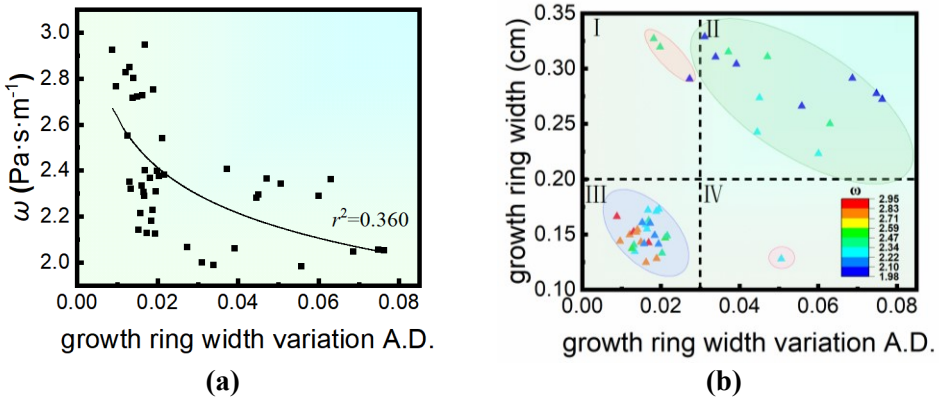

Figure 12. (a) Effect of growth ring width variation *A.D.* on ω; **(b)** effect of growth ring width and growth ring width variation *A.D.* on ω.

The increase in the inhomogeneity of the width variation makes the internal structure of the wood more disordered and the density distribution more uneven. Overall, the average density of the wood is relatively low, and the value of ω decreases. Since the fitting correlation coefficient in **Figure 12a** is relatively low, and considering that the growth ring width of the specimen will have a certain impact on

it, the growth ring width of the specimen is added as a reference in **Figure 12b**. It can be seen from **Figure 12b** that the values of ω in zones I and II are generally smaller than those in zone III, indicating that the growth ring width has a significant impact on the value of ω of the specimen. A larger width corresponds to a smaller acoustic impedance. When the growth ring width of the specimens in zone III is within the range from 0.14 cm to 0.18 cm and the average deviation of the width variation is within the range from 0.016 to 0.020, the ω value of the specimens is relatively small. During vibration, the sound has a higher propagation efficiency, and the timbre is richer and brighter.

The relationship between the average deviation of the variation of growth ring width and tan δ is shown in **Figure 13a**, and the relationship between the growth ring width of the specimen, the average deviation of the variation of growth ring width, and tan δ is shown in **Figure 13b**.

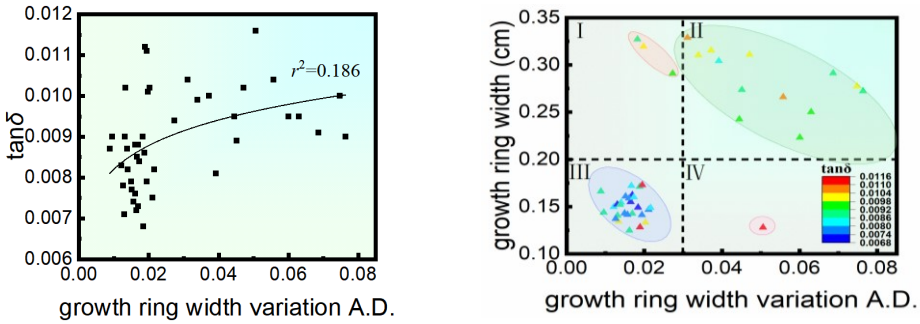

(a) **(b)**

Figure 13. (a) Effect of growth ring width variation *A.D.* on tan δ; (**b**) effect of growth ring width variation *A.D.* on tan δ.

It can be seen in **Figure 13a** that the value of tan δ tends to increase as the degree of inhomogeneity in the growth ring width distribution increases. The increase in the inhomogeneity of the width variation makes the internal structure of the wood more disordered. During vibration, the significantly different vibration characteristics interact with each other, and the vibration energy is lost due to friction, resulting in an increase in tan δ. Since the fitting correlation coefficient in **Figure 13a** is relatively low, and considering that the growth ring width of the specimen will have a certain impact on it, the growth ring width of the specimen is added as a reference in **Figure 13b**. It can be seen in **Figure 13b** that the mean value of tan δ of the specimen in zone III is smaller than that of the other three zones. It indicates that the specimen with smaller and more uniformly distributed growth ring width has less internal friction loss during vibration and better acoustic vibration performance. Moreover, in zone III, when the growth ring width of the specimen is within the range of 0.14 cm to 0.18cm and the average deviation of the width is within the range of 0.008 to 0.020, the tan δ value of the specimen is the smallest. At this time, the vibration attenuation of the wood is slow, which can produce a longer lingering sound and a sustained effect, making the timbre softer and warmer and providing a comfortable auditory experience.

3.3. Effect of latewood rate inhomogeneity on acoustic vibration performance

The relationship between the average deviation of latewood rate and E/ρ is shown in **Figure 14a**, and the relationship between latewood rate, average deviation of latewood rate, and E/ρ of the specimens is shown in **Figure 14b**.

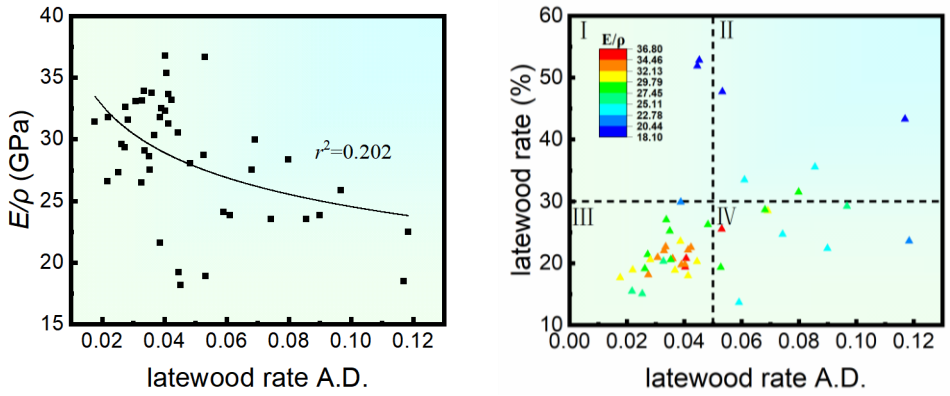

(a) **(b)**

Figure 14. (a) Effect of latewood rate *A.D.* on E/ρ; **(b)** effect of latewood rate, latewood rate *A.D.*, on E/ρ.

Figure 14a shows that with the increase in the inhomogeneity degree of the latewood rate, the E/ρ value of the specimen has a tendency to decline. Due to the change of the growth environment, there is a significant difference in the cell structure between the earlywood and the latewood of the wood. The cell cavities of the latewood are small while the cell walls are thick, resulting in a relatively high density. In contrast, the earlywood has large cell cavities and thin cell walls, with a lower density. As the inhomogeneity of the latewood rate increases, the variability of the proportion of earlywood and latewood within different growth rings also increases, leading to a greater difference in density. When the wood vibrates, the vibration anisotropy in regions with different densities increases, the energy transfer efficiency decreases, and the value of E/ρ reduces. Since the fitting correlation coefficient in **Figure 14a** is relatively low, and considering that the latewood rate of the specimen has a certain impact on it, the latewood rate of the specimen is added as a reference in **Figure 14b**, and the axes are divided into four zones. In zone I, the latewood rate deviation ranges from 0 to 0.05, and the latewood rate ranges from 30% to 60%. In zone II, the deviation ranges from 0.05 to 0.12, and the latewood rate ranges from 30% to 60%. In zone III, the deviation ranges from 0 to 0.05, and the latewood rate ranges from 10% to 30%. In zone IV, the deviation ranges from 0.05 to 0.12, and the latewood rate ranges from 10% to 30%. It can be seen that the specimens are mainly distributed in zones III and IV, where the latewood rate is within 30%. The mean value of E/ρ of the specimens in zone III is higher than that of the other three zones, which indicates specimens with lower latewood rate and more uniform distribution have higher vibration efficiency. When the latewood rate of the specimens within zone III is in the range of 15% to 25% and the average deviation of the latewood rate is within the range of 0.03 to 0.045, the E/ρ value of the specimens is the largest. During vibration, the sound features a richer and brighter timbre. The results are consistent with previous studies indicating that

when the latewood rate of wood is within the range of 15% to 28%, the wood exhibits excellent acoustic properties [16]. This shows that the research results are relatively accurate, and the introduction of image processing technology can enable the precise extraction of the characteristic values of wood grain.

The relationship between the average deviation of latewood rate and *R* is shown in **Figure 15a**, and the relationship between latewood rate, average deviation of latewood rate, and *R* of the specimens is shown in **Figure 15b**.

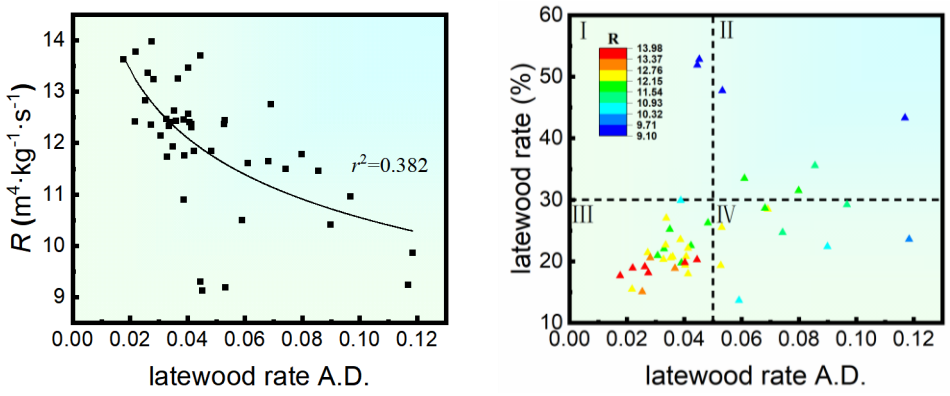

(a) **(b)**

Figure 15. (a) Effect of latewood rate *A.D.* on *R*; **(b)** effect of latewood rate, latewood rate *A.D.* on *R*.

It can be seen in **Figure 15a** that the value of *R* decreases with the increase in the degree of inhomogeneity of the latewood rate. As the inhomogeneity of the latewood rate increases, the variability of the wood's microstructure also increases. When the wood vibrates, the vibration anisotropy in different regions becomes more pronounced, which is unfavorable for the directional radiation of sound, resulting in a decrease in the value of *R*. Since the fitting correlation coefficient in **Figure 15a** is relatively low, and considering that the latewood rate of the specimen has a certain impact on it, the latewood rate of the specimen is added as a reference in **Figure 15b**. The *R* value of the specimens in zone III is higher than that of the other three zones. It indicates that the specimens with a lower latewood rate and more uniform latewood rate have higher sound power radiated to the surrounding air during vibration and better acoustic performance. Within zone III, when the latewood rate is in the range of 15% to 20% and the average deviation of the latewood rate is within the range of 0.02 to 0.048, the value of *R* of the specimen is the largest. At this time, the sound of the wood's vibration has a stronger sense of space and hierarchy, and the sound expression ability is better.

The relationship between the average deviation of latewood rate and ω is shown in **Figure 16a**, and the relationship between latewood rate, average deviation of latewood rate, and ω for the specimens is shown in **Figure 16b**.

The pattern between the latewood rate inhomogeneity and the value of ω is observed to be less obvious in **Figure 16a**. Although the inhomogeneity of the latewood rate increases and the inhomogeneity of the wood density also increases, due to the relatively complex calculation of the average density of the wood, there is no obvious change trend following the variation of the inhomogeneity of the latewood

rate. The value of ω of the wood is positively correlated with its density, resulting in no obvious pattern between the variation of the inhomogeneity of the latewood rate and the value of ω of the wood. The latewood rate of the specimens added in **Figure 16b** is analyzed, and the ω values are generally small in the four regions. Fewer specimens have larger ω values in regions III and IV, concentrating in the range of 0.03 to 0.06 of the latewood rate's average deviation. There was no significant pattern of influence between latewood rate inhomogeneity and ω value.

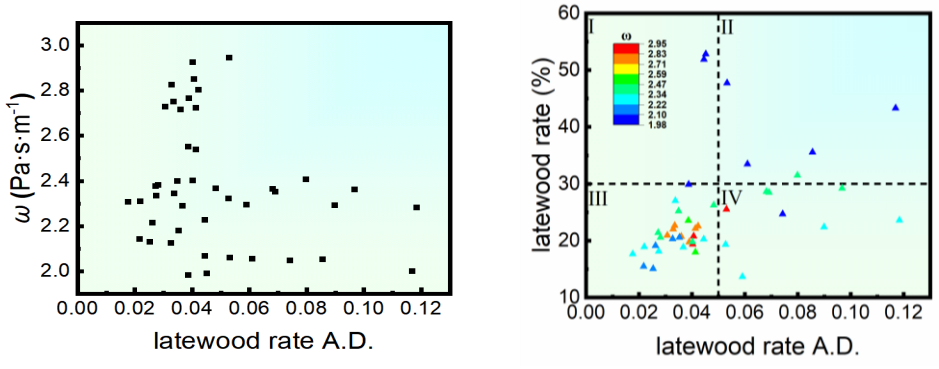

(a) **(b)**

Figure 16. (a) Effect of latewood rate *A.D.* on ω; **(b)** effect of latewood rate, latewood rate *A.D.* on ω.

The relationship between the average deviation of latewood rate and tanδ is shown in **Figure 17a**, and the relationship between the latewood rate, the average deviation of latewood rate, and tanδ of the specimens is shown in **Figure 17b**.

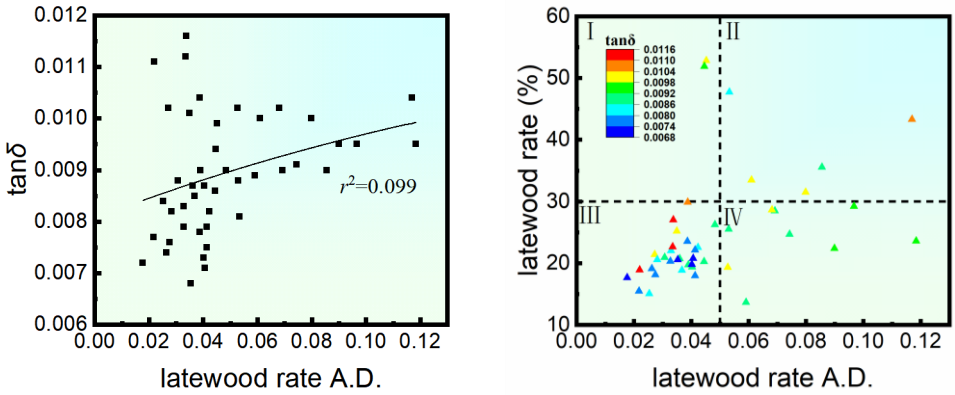

(a) **(b)**

Figure 17. (a) Effect of latewood rate *A.D.* on tan δ; **(b)** effect of latewood rate, latewood rate *A.D.* on tan δ.

In **Figure 17a**, the tan δ value tends to increase with the rise of the latewood rate's average deviation. As the inhomogeneity of the latewood rate increases, the difference in the cell wall structure among different latewood regions becomes larger. When the wood vibrates, the anisotropy increases, the internal friction loss rises, and the value of tan δ increases. Since the fitting correlation coefficient in **Figure 17a** is relatively low, it is considered that the latewood rate of the specimen has a certain influence on it. In **Figure 17b**, the latewood rate of the specimen is added for analysis,

and it can be clearly seen that the tan δ value of the specimen in zone III is smaller than that of the other three zones. It indicates that the specimen with a lower latewood rate and a more uniform latewood rate has less internal friction loss during vibration and better acoustic vibration performance. Among them, the specimens with the latewood rate within the range of 15% to 20% and the average deviation of the latewood rate within the range of 0.02 to 0.048 have the smallest tan δ value. At this time, the vibration attenuation of the wood is slow, which can produce a longer lingering sound and a sustained effect, making the timbre softer and warmer.

4. Discussion

This study has accurately extracted the grain characteristics of wood using image processing technology and deeply explored the influence rules of the inhomogeneity of growth ring width, growth ring width variation, and latewood rate on the acoustic parameters of wood. The research shows that as the inhomogeneity of the growth ring width and the inhomogeneity of the variation in the growth ring width increase, the values of E/ρ, R, and ω of the wood decrease, while the value of tan δ increases. Meanwhile, the increase in the inhomogeneity of the latewood rate leads to a decrease in the values of E/ρ and R of the wood and an increase in the value of tan δ. However, the inhomogeneity of the latewood rate has no significant effect on the value of ω.

As a natural material, wood has an internal structure whose complexity determines its acoustic properties. The inhomogeneity of growth ring width, growth ring width variation, and latewood rate implies that there are significant differences in the internal cell structure, cell wall thickness, etc., of the wood. The inhomogeneity of the structure will cause an increase in the anisotropy of the vibration characteristics of the wood, resulting in low vibration efficiency and large energy loss. Consequently, the values of E/ρ and R decrease, and the value of tan δ increases. However, through analysis, it was found that the correlation coefficients between the inhomogeneity of the wood grain and E/ρ, R, and tan δ are relatively low. This may be because the wood specimens themselves have a large degree of variability, and their internal microstructures are complex and difficult to control. In addition, the current research only measures the macroscopic characteristic values of the wood specimens. This approach has significant limitations and is difficult to comprehensively reflect the factors affecting the above-mentioned acoustic parameters, thus resulting in poor performance of the correlation between the inhomogeneity of the wood grain and these parameters. In the follow-up, the micro-density measurement technique can be used to deeply explore the density at different positions of the wood grain characteristics, more accurately characterize the internal structural changes of the inhomogeneous wood grain, and make the research results more scientific and accurate. Meanwhile, the wood's ω is positively correlated with its density. However, as the calculation of wood's average density is complex and shows no clear trend with the variation in latewood rate inhomogeneity, this study failed to determine how the inhomogeneity of the latewood rate affects ω. In subsequent research, measuring the micro-density of the wood can improve this part of the content.

Previous studies have focused on the relationship between the macroscopic characteristics of wood and its acoustic properties, but the research methods in terms

of the quantitative analysis of grain characteristics and their correlation with acoustic parameters are relatively single. Similar to this study, some studies have found that the inhomogeneity of wood grain has a negative impact on the acoustic properties [17,18,34]. However, this study has achieved the accurate extraction of the characteristic values of wood grain by using image processing technology, making improvements in the research method. At the same time, this study clearly indicates that when the growth ring width is within the range of 0.14 cm to 0.17 cm, the deviation of the growth ring width is within the range of 0.024 to 0.036, and the deviation of the variation in the growth ring width is within the range of 0.016 to 0.020, the wood has the best acoustic vibration performance. Such precise quantitative relationships are important supplements and expansions to the existing research.

Meanwhile, wood with uniform grain not only has better acoustic properties but may also possess higher mechanical stability and durability. During the vibration process, wood is continuously subjected to periodic stress. The inhomogeneity of the grain can lead to a more complex stress distribution inside the wood, and the stress amplitude in some areas may be significantly higher. Under long-term vibration, the areas with high stress amplitude are more prone to fatigue damage, such as the propagation of micro-cracks in the cell walls. This fatigue damage accumulates over time, reducing the mechanical strength and stiffness of the wood. This means that wood with uniform grain can better maintain its acoustic properties and structural integrity during long-term use.

Although this study has achieved certain results, there are still some limitations. Firstly, although the image processing technology can extract the grain characteristics of wood, it is unable to effectively obtain some microscopic structural characteristics, which may affect the comprehensive understanding of the influencing mechanism of the acoustic properties. Secondly, the types of wood samples selected in the experiment are limited, which may restrict the universality of the research results for a wider variety of wood species. In addition, only the acoustic vibration parameters were used to characterize the acoustic properties of wood, and there was no more intuitive exploration of the timbre of the wood.

Based on the limitations of this study, future research can be carried out in the following directions. On the one hand, advanced microscopic analysis technologies, such as the combination of scanning electron microscopy (SEM) and image processing technology, can be integrated to deeply explore the relationship between the microscopic structure of wood and its grain characteristics and their influence mechanism on the acoustic properties. On the other hand, the types and sources of wood samples should be expanded to improve the universality of the research results. Moreover, the intuitive analysis of the timbre of wood should be added to make the experimental results more scientific.

5. Conclusion

Clear and accurate identification of the boundaries between earlywood and latewood was enabled by using MATLAB image processing technology. Meanwhile, Digimizer software facilitated the accurate measurement of growth ring width and latewood rate. By integrating advanced image processing techniques with traditional

wood science theories, a comprehensive and accurate understanding of wood grain characteristics can be achieved.

The inhomogeneity of the grain has a certain influence on the acoustic properties of wood. As the inhomogeneity of the growth ring width and the variation in the growth ring width increase, the values of E/ρ, R, and ω of the wood decrease, while the value of tan δ increases. As the inhomogeneity of the latewood rate increases, the values of E/ρ and R of the wood decrease, and the value of tan δ increases. The inhomogeneity of the latewood rate has no significant effect on ω. The variation patterns of these acoustic parameters indicate that wood with a uniform grain has better acoustic properties.

By jointly analyzing the growth ring width of the wood and the latewood rate and comprehensively considering the performance of E/ρ, R, tan δ, and ω, it can be concluded that when the growth ring width is within the range of 0.14 cm to 0.17 cm, the deviation of the growth ring width is within the range of 0.024 to 0.036, and the deviation of the variation in the width is within the range of 0.016 to 0.020, the values of E/ρ and R of the wood are the largest, and the values of ω and tan δ are the smallest, indicating the best acoustic vibration performance. When the latewood rate is within the range of 15% to 20% and the deviation of the latewood rate is within the range of 0.03 to 0.045, the values of E/ρ and R of the wood are the largest, and the value of tan δ is the smallest, meaning the best acoustic vibration performance of the wood.

Instrument manufacturers have always been committed to finding woods with excellent acoustic properties in order to create musical instruments with outstanding timbres. This study clearly indicates the range of texture variations within which the acoustic vibration performance of wood is optimal. This provides instrument manufacturers with precise material selection criteria, enabling them to screen out the most suitable materials for making musical instruments from a large number of woods, thus improving the sound quality and overall quality of the instruments. For example, when making a violin, manufacturers can select woods according to these criteria, and the violins produced may have a richer timbre, higher resonance, and better acoustic response.

Overall, this study introduced image processing technology to accurately extract the grain characteristics of wood and explored the influence of the inhomogeneity of wood grain on the acoustic vibration performance of wood, which can provide a theoretical reference for the rational selection of materials for subsequent musical instruments.

Author contributions: Conceptualization, SW and ZL; methodology, SW, ZL and YH; software, SW, YH and XL; validation, SW, JZ (Juncheng Zhang) and YG; formal analysis, JZ (Juncheng Zhang) and YG; investigation, SW and LH; resources, SW and JZ (Jing Zhou); data curation, SW and XL; writing—original draft preparation, SW; writing—review and editing, SW, JZ (Juncheng Zhang) and YG; visualization, SW and XL; supervision, ZL and YH; project administration, ZL; funding acquisition, ZL. All authors have read and agreed to the published version of the manuscript.

Funding: This research was funded by the National Natural Science Foundation of China, grant numbers 32271781; and the Fundamental Research Funds for the Central

Universities, grant number 2572021AW54.

Institutional review board statement: Not applicable.

Informed consent statement: Not applicable.

Conflict of interest: The authors declare no conflict of interest.

References

1. Liu Z, Liu Y. Research Status and Prospect of Acoustic Vibration Properties Modification of Wood Used for Soundboard (Chinese). World Forestry Research. 2012; 25(01): 44–48.
2. Tang Q, Wang Y. Study on Acoustic Vibration Properties of Wood and Bamboo for Musical Instruments (Chinese). Paper Science & Technology. 2024; 43(06): 24–27.
3. Rolleri A, Wentzel M, Aguilera A, et al. Vibroacoustic Properties as a Function of Crystallinity Changes in Heat-Treated Pinus Radiata D. Don Wood. Wood Material Science & Engineering. 2024; 19(01): 247–252.
4. Liu M, Peng L, Lü S, et al. Acoustic Vibration Analysis of Tropical Hardwoods for Fretboard of String Musical Instrument. Scientia Silvae Sinicae (Chinese). 2021; 57(06): 125–133.
5. Wan K, Zhou J, Zhang H, et al. Effect of Crack Length on Acoustic Vibration Properties of Paulownia Wood. Journal of Forestry Engineering (Chinese). 2023; 8(05): 55–62.
6. Zhang L, He L, Liang Y, et al. Modulating the Acoustic Vibration Performance of Wood by Introducing a Periodic Annular Groove Structure. Forests. 2023; 14(12): 2360.
7. Nop P, Tippner J. Influence of Dimensions of Wooden Samples for Determination of Acoustic Parameters and Sound Timbre. Applied Acoustics. 2022; 196(6): 108895.
8. Zhao X, Liu Y, Zhao L, et al. A Scalable High-Porosity Wood for Sound Absorption and Thermal Insulation. Nature Sustainability. 2023; 6(2): 306–315.
9. Wang R, Liu Y, Hu J, et al. Visual Characteristics of Wood Tangential Section Pattern (Chinese). Journal of Central South University of Forestry & Technology. 2022; 43(01): 181–190.
10. Dinulica F, Stanciu MD, Savin A. Correlation between Anatomical Grading and Acoustic-Elastic Properties of Resonant Spruce Wood Used for Musical Instruments. Forests. 2021; 12(8): 1122.
11. Dinulica F, Savin A, Stanciu MD. Physical and Acoustical Properties of Wavy Grain Sycamore Maple (Acer Pseudoplatanus L.) Used for Musical Instruments. Forests. 2023; 14(2): 197.
12. Zhang C, Xu W, Wu Z, et al. Effects of Annual Rings Direction on Acoustical Property of Spruce Wood Used for the Soundboard of Piano (Chinese). Journal of Nanjing Forestry University (Natural Sciences Edition). 2010; 34(3): 165–167.
13. Tao X, Han J, Xu W, et al. Effect of Spruce Grain Angle on Acoustic Vibration Properties of Piano Soundboard (Chinese). Chinese Journal of Wood Science and Technology. 2019; 33(4): 14–17.
14. Guiman MV, Stanciu MD, Roșca IC, et al. Influence of the Grain Orientation of Wood upon its Sound Absorption Properties. Materials. 2023; 16(17): 5998.
15. Liu Z, Li S, Liu Y, Huang Y. Vibration Modal Analysis of Resonance Board of Ruan and Yukin (Chinese). Journal of Northeast Forestry University. 2011; 39(12): 74–76.
16. Liu Y, Shen J, Tian Z, et al. Study on Relationship between Sound Vibration Parameters and Growth Ring Width and Latewood Percentage of Picea Genera Wood (Chinese). Scientia Silvae Sinicae. 2001; 37(6): 86–91.
17. Shen J, Liu Y, Liu M, et al. Effects of Variance Coefficient of Growth Ring Width on Sound Vibration Parameters of Picea Wood (Chinese). Journal of Northeast Forestry University. 2005; 33(5): 27–29.
18. Shen J, Liu Y, Liu M. Variance Coefficient of Latewood Percentage to Sound Vibration Parameters of Picea Genera Wood (Chinese). Journal of Fujian College of Forestry. 2005; 25(3): 225–228.
19. Viala R, Cabaret J, Sedighi-Gilani M, et al. Effect of Indented Growth Rings on Spruce Wood Mechanical Properties and Subsequent Violin Dynamics. Holzforschung. 2024; 78(3): 189–201.
20. Xie C, Yang B, Li R. Wood Defect Detection Method Based on Double Least Generative Adversarial Networks and Dense-Net (Chinese). Journal of Forestry Engineering. 2023; 8(04): 129–136.
21. Cheng Y, Cai Y. Wood Defect Image Segmentation Algorithm Based on Fractional Order CV Model (Chinese). Forestry Machinery & Woodworking Equipment. 2018; 46(04): 44–47+51.

22. Zamri MIP, Cordova F, Khairuddin ASM, et al. Tree Species Classification Based on Image Analysis Using Improved-Basic Gray Level Aura Matrix. Computers and Electronics in Agriculture. 2016; 124: 227–233.
23. Cheng Y, Li Z, Sun Y. Detection Algorithm of Wood Rings Image Based on Texture Feature (Chinese). Forest Engineering. 2018; 34(03): 46–49+92.
24. Nedzved A, Mitrovic AL, Savic A, et al. Automatic Image Processing Morphometric Method for the Analysis of Tracheid Double Wall Thickness Tested on Juvenile Picea Omorika Trees Exposed to Static Bending. Trees-Structure and Function. 2018; 32(5): 1347–1356.
25. Yu H, Pan S, Zhang Y. Mesoscale Modeling Method for Flexural Modulus of Larch (Chinese). Journal of Northeast Forestry University. 2018; 46(12): 108–111.
26. Li H, Zhou G, Wang C. Detection of Irregularity Crack Based on MATLAB Image Processing Toolbox (Chinese). Computer Engineering and Applications. 2016; 52(05): 209–214+219.
27. Fang H, Chen H, Jiang H, et al. Research on Method of Farmland Obstacle Boundary Extraction in UAV Remote Sensing Images. Sensors. 2019; 19(20): 4431.
28. Hu J, Song W, Zhang W, et al. Deep Learning for Use in Lumber Classification Tasks. Wood Science and Technology. 2019; 53(2): 505–517.
29. Sun M. Comparison of Processing Results of Median Filter and Mean Filter on Gaussian Noise. Applied and Computational Engineering. 2023; 5: 779–785.
30. Onim A, Musyoki S, Kihato P. Selection of Optimal Sinr Threshold in Fractional Frequency Reuse by Comparing Otsu's and Entropy Method. Heliyon. 2022; 8(11): e11736.
31. Xu D, Shao Z. Effects of Wood Density on Sound Vibration Parameters (Chinese). Journal of Anhui Agricultural University. 2012; 39(03): 361–364.
32. Liu M, Peng L, Lü S, et al. Research Progress of Wood Treatment to Improve Acoustic Vibration Performance for Making Musical Instruments (Chinese). China Wood Industry. 2020; 34(2): 29–33.
33. Liu Z, Liu Y, Miao Y, et al. Relationship between Vibration Property of Resonance Board and Subjective Evaluation of Piano Acoustical Quality (Chinese). Scientia Silvae Sinicae. 2009; 45(04): 100–106.
34. Qin L, Miao Y, Liu Z. Influence of The Main Pysical Characteristics and Components Content of P. Elongata on Acoustic Vibration Performance (Chinese). Forest Engineering. 2017; 33(04): 34–39.
35. Liang Y, He L, Zhang L, et al. Effect of Oil Heat Treatment on the Acoustic Vibration Performance of Bamboo (Chinese). Forest Engineering. 2024; 40(03): 115–124.